抗体療法の開発に関する研究

分担研究者　竹腰　正隆（東海大学医学部）

研究要旨

HCMV 感染症の予防と治療用のヒト中和抗体作りをめざしている。主要中和抗原を担う gB と gH に対する抗体作りを主として大腸菌の系を用いて得られた Fab 抗体をホール化して植物で産生する系を昨年度構築したが、制限酵素の設定に問題があったため再度、最初から構築を行い、植物でのホール抗体産生ベクターの構築に成功した。

A．研究目的

現在、ヒトサイトメガロウイルス（HCMV）感染症の予防と治療には、アシクロビルやガンシクロビルといった核酸アナログが用いられている。薬剤の活性化にはリン酸化が必要だが HCMV は主要なリン酸化酵素であるチミジンキナーゼ遺伝子を持っていない。このため抗ウイルス剤の効果が他のヘルペスウイル群に比べて弱い。そこでこれらの薬剤とはまったく作用機序の異なる抗ウイルス剤として、ヒト中和抗体を用いることができれば、HCMV 感染症の予防と治療に大きな福音となると考えられる。

これまでのところウイルス中和エピトープを担う抗原としては下記の３種が存在すると言われている。

中和抗原	糖鎖有	糖鎖無
gB（gCI）	UL55 58k-116k	102k
gH（gCIII）	UL75 86k	84k
gN（gCII）	UL73 50～60k	15k

本研究では主として主要中和抗原である gB と gH に対する中和抗体の取得を目指した。一方、中和抗原ではないが液性免疫かく乱系として IgG の Fc 領域に結合することによって抗体を排除する Fc γレセプター遺伝子が近年になって同定された。それは下記の２種である。

Fc γレセプター	糖鎖有	糖鎖無
TRL11	34k	24k
UL119-8	68k	33k

同じヘルペスウイルスグループに属する HSV での研究から、これら Fc γレセプターに対する中和抗体が存在すると、本来のウイルス中和抗体の効果が増大することが知られている。このため本研究では TRL11と UL119-8に対するヒト中和抗体の産生も目指した。

治療用抗体の研究は世界的に盛んに行われている。しかしウイルスに対する抗体の開発はあまり活発とはいえず、実用化されたものは呼吸器感染症の原因となる RSV に対するものだけである。特に HCMV においては中和抗原の多様性が指摘されており、抗体開発には多くの臨床株のデータが必要と思われる。ヒト抗体で有名なアメリカの抗体開発メーカーの研究者の１人は、ウイルスに対する抗体はその知識を保有する大学に責任がある、とまで言う。本研究は HCMV の臨床分離株を多く有する研究者ら（本研究の分担研究者でもある）とのネットワークを活用して、HCMV 感染症の予防と治療に有効なヒト抗体の開発に真摯に取り組むものである。

B．研究方法

研究方法は大きく分けて２つからなる。１つはすでに得られた抗 HCMV 中和ヒト Fab 抗体のホール化である。これは抗体価の高いヒトから得た中和 Fab 抗体をホール抗体（IgG1）に変換し、植物での大量生産を試みるものである。ホール化することにより、中和抗体価の上昇と血中半減期の増大が期待できる。また生産の場として植物を用いることにより、既存の方法よりも安価にかつ大量に抗体を生産できる利点がある。

もう１つの試みは抗原となるタンパク質（中和抗原、Fc γレセプター）のバキュロウイルスの系を用いた生産である。これら抗原が生産できればヒト抗体産生マウスである KM マウスに免疫することにより、ハイブリドーマ法によってヒト抗体を得ることができる。これら抗原を生産するため大腸菌の系を用いたが、膜タンパク特有の構造の複雑さからか、うまく生産することができなかった。またエレクトロポレーションを用いた DNA 導入で KM マウスを直接免疫したが、抗体価の上昇は認められなかった。このため複雑な折りたたみタンパクの産生が可能なバキュロウイルスの系を用いることにした。

１．ヒト抗体の植物発現ベクターの構築

Fab 抗体のうちＬ鎖は全領域が含まれるが、Ｈ鎖に関しては VH-CH1しか含まれず、CH2-CH3を欠いている。そこで我々の研究室ですでにクローニングした抗 HBs 抗体遺伝子 CL4（IgG1）の CH1-CH2-CH3領域を用いてホール化を行う。CH1の5' 側15塩基ほど離れた所に制限酵素の ApaI サイトが存在する。これは IgG1～4まで共通である。したがって、IgG 由来の Fab は VH 領域と隣接する CH1の5' 端を ApaI で切り出し、CL4の CH1-CH3領域の上流にクローニングすることでインフレームに

ホール化することができる。IgG以外のFabの場合はApaIサイトとCH1の5'側15塩基ほどを付加したプライマーでVH領域を増幅して、同じようにCL4のCH1-CH2-CH3領域にクローニングする。

植物発現ベクターとしては共同研究を行っているドイツのフランフォファー研究所の分子生物学応用生態学研究所ライナー・フィッシャー部長から供与されたpTRAkc-ERHをベースに抗体遺伝子のL鎖とH鎖の2つの遺伝子を導入できるように改造する。

2．抗原タンパクのバキュロウイルス系での生産

中和エピトープを担うgB、gHおよびFc γレセプターのTRL11、UL119-8についてバキュロウイルス系での生産を行う。そのためにいずれのタンパク質も本来の分泌シグナルをそのまま利用して、培養液中に分泌させる。また膜貫通ドメインは除去する。タグとしてはHis-TagをC末端に付加し、精製に利用する。バキュロウイルスの感染には一般に用いられるSf9細胞に加え、タンパク産生効率の良いTn5細胞も抗原生産時に用いる。そして、分泌タンパク質の精製を容易にするため無血清培地で培養する。以上の条件で産生を試みる。使用する組換えバキュロウイルス作製用インサーションベクターはInvitrogen社のpFastBac1とPharmingen社のpVL1392である。前者はバキュロウイルスゲノムがBacmidの形で大腸菌に入ってるため、大腸菌内で組換えが行える（Bac to Bacシステム）。後者は欠損したバキュロウイルスゲノムと一緒にトランスフェクションしてSf9細胞で組換え体を作製する。

C．研究結果

1－1．植物発現ベクターの再構築

ベクターの出発材料としてpBluescript（pBs）を用いた。まずpBsのマルチクローニングサイトのsalIサイトを切断した後に平滑化してライゲーションを行い、結果的にsalIサイトを消失させた。次にPstI-SpeI間に合成リンカーを導入して植物用分泌シグナルとなるLPH配列を導入した。この配列は使用予定のタバコのコドン使用頻度に合わせて塩基配列を最適化した。さらに分泌シグナルが適切に切り出されるかどうかをデンマーク工科大学の予測サイト（http://www.cbs.dtu.dk/services/SignalP/）を用いて検定した。同時に制限酵素サイトのPstIサイトを消失させ、SpeIサイトをNheIサイトに変換した。次にLPHの5'側のXhoI-EcoRIサイトにpTRAkc-ERH由来の植物用プロモーターの0.7kbを導入した後にEcoRIサイトを消失させた。次にLPHの3'側のXbaI-SacIIサイトにpTRAkc-ERH由来の植物用polyAシグナルの0.3kbを導入した。得られたベクターをpPLA2と名付けた。これをL鎖用とH鎖用に分けるために、pPLA2の5'側にあるApaIサイトと3'側にあるSacIサイトをそれぞれL鎖用にEcoRI-NotIサイト、H鎖用にAscI-HindIIIサイトに変換した。これらベクターに関してもシークエンシングを行い塩基配列の確認を行った。L鎖とH鎖を植物に導入するために次に植物導入用ベクターpTRAkc-ERHの改造を行った。pTRAkc-ERHのAscI-FseI領域を切り出し、代わりにAscI-HindIII-EcoRI-NotI-FseIlikeサイトを含む合成リンカーを導入し、pTRAkc-ANと名付けた。これによりFab抗体をIgG1に変換して植物で発現させるために必要なすべてのベクターが完成した。

現在、このベクターにHCMV中和抗体遺伝子である13-3とTG252の遺伝子を導入した。抗体遺伝子のホール化はシークエンシングによって確認した。今後、植物細胞による抗体の産生に挑戦する。

2．抗原タンパクの産生

2－1．gHの産生

gHタンパクの膜貫通ドメインの直前、アミノ酸で1-750番までの領域をPCRで増幅しバキョロウイルスに導入して発現させた。Invitrogen社のpFastBac1よりPharmingen社のpVL1392の方が産生効率が良かったので、pVL1392を用いて産生条件を検討している。産生の確認はgHを認識するマウスモノクローナル抗体を用いてウエスタンブロットで行った。予想される分子量よりも若干低かったので、現在その理由について調べている。

2－2．Fc γレセプターの産生

Fc γレセプターに関しては既存の抗体がないためHis-Tagに対する検出法でその産生を確認した。TRL11に比べUL119-8の方が産生量が多かったので、UL119-8の生産を先に進め、現在までに数ミリグラムを産生した。TRL11に関しては2ミリグラムを生産した。これらを濃度を変えてELISAプレートに塗布し、ヒトIgGとそのFabを反応させたところ、TRL11もUL119-8も濃度依存的にIgGのみと特異的に反応し、Fabとはまったく反応しないことを確認した。まちがいなくFc γレセプターであると思われる。

現在、大量培養、大量精製法について種々の検討を行っているが、培養細胞にSf9を用いフラスコを用いた振盪培養が効率よく生産できている。

D．考　察

Fabホール化ベクターおよび植物発現ベクターに関しては、1度は完成したが、制限酵素の設定に不備があり、再度設計をやりなおした。ベクターはすべて完成し、シークエンシングによって設計通りに構築されたことが確認された。実際に目的の抗体遺伝子（13-3、TG252）をホール化して発現ベクターにクローニングしたが、シークエンシングの結果、目的通りに遺伝子の構築が出来ていた。これらの抗体遺伝子にはL鎖とH鎖に両方にKDEL配列と呼ばれるシグナル配列を付加した物と付加しない物の2種類を構築した。KDEL配列を付加するとタンパクの小胞体への輸送が促進される事が知られていて、結果的に分泌タンパクの生産増大が期待できる。この点に関し抗体の生産量に変化が有るかどうかの検討を行う。

抗原タンパクの産生に関しバキュロウイルスの系においての産生が順調に進み、現在それらを用いてマウスに

免疫を試みている。もしマウスで抗体が得られるようならヒト抗体産生マウスであるKMマウスでの免疫を試み、ヒト抗体を取る予定である。また得られたマウス抗体による抗原の解析も試みたい。

E．結　　論

HCMV感染症の予防と治療に用いるヒト中和抗体を作るために、抗体産生用に用いる2種のベクターの再構築を行った。それらのベクターを用いて抗体の遺伝子のホール化とクローニングが問題なく行えることを確認した。また抗原タンパクの生産もバキュロウイルスの系で順調に進んでいる。中和抗原を担うgBタンパクだけではなく、gHタンパクの生産にも成功した。中和抗体の働きを妨害するFc γレセプターの産生もUL119-8に続いてTRL11についても成功した。今年度も予定通りの進捗状況であり、計画通りに研究が遂行できると確信している。

F．研究発表

1．論文発表

1）Murayama T, Takekoshi M, Tanuma J, Eizuru Y: Analysis of human cytomegalovirus UL144 variability in low-passage clinical isolates in Japan. Intervirology 48: 201-6, 2005

2）Maeda F, Takekoshi M, Nagatsuka Y, Aotsuka S, Tsukahara M, Ohshima A, Kido I, Ono Y, Ihara S: Production and characterization of recombinant human anti-HBs Fab antibodies. J Virol Methods 127: 141-7, 2005

3）Kitaguchi K, Toda M, Takekoshi M, Maeda F, Muramatsu T, Murai A: Immune deficiency enhances expression of recombinant human antibody in mice after nonviral in vivo gene transfer. Int J Mol Med 16: 683-8, 2005

4）矢野　明，竹腰正隆：植物でヒトの抗体を作る．バイオニクス　2：32-8, 2005

2．学会発表

なし

G．知的財産権の出願・登録状況

1．特許取得

なし

2．実用新案登録

なし

3．その他

なし

Ⅲ. 研究成果の刊行に関する一覧表

雑　誌

発表者氏名	論文タイトル名	発表誌名	巻号	ページ	出版年
Kanemaru S, Nakamura T, Omori K, Magrufov A, Yamashita M, Ito J	Regeneration of mastoid air cells in clinical applications by in situ tissue engineering	Laryngoscope	115(2)	253～258	2005
Tsuchiya E, Oki J, Yahara N, Fujieda K	Computerized version of the Wisconsin card sorting test in children with high-functioning autistic disorder or attention-deficit/hyperactivity disorder	Brain Dev	27	233～236	2005
Yokota S, Yokosawa N, Okabayashi T, Suzutani T, Fujii N	Induction of suppressor of cytokine signaling-3 by herpes simplex virus type 1 confers efficient viral replication	Virology	338	173～181	2005
Kaneko H, Iida T, Aoki K, Ohno S, Suzutani T	Sensitive and rapid detection of herpes simplex virus and varicella-zoster virus DNA by loop-mediated isothermal amplification	J Clin Microb	43	3290～3296	2005
Saijo M, Suzutani T, Morikawa S, Kurane I	Genotypic characterization of the DNA polymerase and sensitivity to antiviral compounds of foscarnet resistant herpes simplex virus type 1 (HSV-1) derived from a foscarnet-sensitive HSV-1 strain	Antimicrob Agents Chemother	49	606～611	2005
Kosugi I, Kawasaki H, Tsuchida T, Tsutsui Y	Cytomegalovirus infection inhibits the expression of N-methyl-D-aspartate receptors in the developing mouse hippocampus and primary neuronal cultures	Acta Neuropathol (Berl)	109(5)	475～482	2005
Tsutsui Y, Kosugi I, Kawasaki H	Neuropathogenesis in cytomegalovirus infection: indication of the mechanisms using mouse models	Rev Med Virol	15(5)	327～345	2005
Han GP, Miura K, Ide Y, Tsutsui Y	Genetic analysis of JC virus and BK virus from a patient with progressive multifocal leukoencephalopathy with hyper IgM syndrome	Journal of Medical Virology	76	398～405	2005
Murayama T, Takekoshi M, Tanuma J, Eizuru Y.	Analysis of human cytomegalovirus UL144 variability in low-passage clinical isolates in Japan	Intervirology	48	201～206	2005
Maeda F, Takekoshi M, Nagatsuka Y, Aotsuka S, Tsukahara M, Ohshima A, Kido I, Ono Y, Ihara S	Production and characterization of recombinant human anti-HBs Fab antibodies	J Virol Methods	127	141～147	2005
Kitaguchi K, Toda M, Takekoshi M, Maeda F, Muramatsu T, Murai A	Immune deficiency enhances expression of recombinant human antibody in mice after nonviral in vivo gene transfer	Int J Mol Med	16	683～688	2005
Wang G, Xu H, Wang Y, Gao X, Zhao Y, He C, Inoue N, Chen HD	Higher prevalence of human herpesvirus 8 DNA sequence and specific IgG antibodies in patients with pemphigus in China	J Am Acad Dermatol	52(3)	460～467	2005

発表者氏名	論文タイトル名	発表誌名	巻号	ページ	出版年
Katano H, Ito K, Shibuya K, Saji T, Sato Y, Sata T	Lack of human herpesvirus 8 infection in lungs of Japanese patients with primary pulmonary hypertension	J Infect Dis	191	743～745	2005
Katano H, Hogaboam CM	Herpesvirus-associated pulmonary hypertension?	American Journal of Respiratory and Critical Care Medicine	172	1485～1486	2005
Asahi-Ozaki Y, Sato Y, Kanno T, Sata T, Katano H	Quantitative analysis of Kaposi sarcoma-associated herpesvirus(KSHV) in KSHV-associated diseases	The Journal of Infectious Diseases	193	773～782	2006
馬場陽子 , 小川　洋 , 大森孝一	保存臍帯より先天性サイトメガロウイルス感染症が診断された難聴乳幼児の聴力像	Audiology Japan	48(5)	315～316	2005
矢野　明 , 竹腰正隆	＜特集 植物の力をバイオ産業に＞ 抗体医薬は植物で	Bionics	2	38～44	2005
井上直樹 , 野澤直樹	＜βヘルペスウイルスの分子生物学＞ HCMV のゲノム構造と遺伝子機能	日本臨牀〔ヘルペスウイルス学 —基礎・臨床研究の進歩—〕	64 (増刊3)	377～385	2006
野澤 直樹 , 井上 直樹	＜βヘルペスウイルス感染症発症機構＞ CMV の先天性感染機構	日本臨牀〔ヘルペスウイルス学 —基礎・臨床研究の進歩—〕	64 (増刊3)	446～450	2006

関連する刊行物

福島県新生児聴覚検査事業	新生児聴覚スクリーニング検査のお知らせ

Ⅳ. 研究成果の刊行物・別刷

The Laryngoscope
Lippincott Williams & Wilkins, Inc.

Regeneration of Mastoid Air Cells in Clinical Applications by In Situ Tissue Engineering

Shin-ichi Kanemaru, MD, PhD; Tatsuo Nakamura, MD, PhD; Koichi Omori, MD, PhD; Akhmar Magrufov, MD; Masaru Yamashita, MD; Juichi Ito, MD, PhD

Objectives: **To regenerate of the mastoid air cells and their functions for the treatment of incurable otitis media.** ***Materials and Method:*** **In situ tissue-engineered mastoid air cells using three-dimensional hydroxy apatite (3D-HA) of honeycomb-like structure were used as artificial pneumatic bones. This 3D-HA is made of calcium phosphate and has a high ratio of micropores, 90%. Its surface is coated with collagen. Ten patients (4 males, 6 females) for this clinical study were randomly selected among the patients with severe cholesteatoma, adhesive otitis media, and purulent chronic otitis media, and they were to be received a staged operation. At the first stage of tympanoplasty, collagen-coated 3D-HA was put into the newly opened mastoid cavity, and it was fixed by fibrin glue. Recovery of mastoid aeration and regeneration of the pneumatic air cells of the mastoid cavity were estimated by images of high-resolution computed tomography (HRCT) after the first operation. At the second stage of operation, histopathologic examinations of specimens of HA taken from the reopened mastoid cavity were performed.** ***Results:*** **Aerations in the mastoid cavity were observed in 9 of the 10 patients within 12 months after the second operation. Moreover, the pneumatic structure in the mastoid cavity was partially regenerated in five patients. In these successful cases, mucosa with newly formed capillaries was observed on the surface of the implanted HA at the second stage of operation. In the failure cases, however, connective tissues and granulations invaded the space of the 3D-HA. They were observed as soft-tissue density areas in the HRCT scan images.** ***Conclusions:*** **This study indicates that mucosa can grow on the surface of implanted artificial 3D-HA and can have a gas exchange function in the newly opened mastoid cavity. These tissue-engineered mastoid air cells may be a possible treatment for intractable otitis media.** ***Key Words:*** **Regeneration of mastoid air cells, gas exchange function, mastoid aeration, three-dimensional hydroxy apatite, collagen coat, intractable otitis media.**

Laryngoscope, **115:253–258, 2005**

INTRODUCTION

Pneumatic bones found in the temporal region have a unique structural feature in that they have a honeycomb-like framework and the inner surfaces of their air cells are covered with a thin mucosa. This structural feature is intimately associated with their physiologic functions. Recent studies have revealed that mastoid air cells, because of the gas exchange function of their mucosa, play an important role in pressure regulation of the middle ear.[1–7] Failure of this function precludes good aeration of the middle ear cavity.

The maintenance of middle ear pressure at the atmospheric level, required for good sound conduction, is one of the most important functions of the mastoid air cell system. Once this function fails, otitis media follows a protracted course.

Tympanoplasty is the best treatment for chronic otitis media. However, there are other, incurable types of otitis media, such as adhesive otitis media and severe cholesteatoma. The common anatomic feature in these cases is the poor development of mastoid air cells, resulting in little or no aeration of the mastoid cavity (Fig. 1). As mentioned above, the failure of pressure regulation in the middle ear is thought to be a possible concern in cases of incurable otitis media.[3,8,9]

We focused on the failure of the gas exchange mechanism in mastoid air cells as a possible cause of intractable otitis media. For regeneration of mastoid cavity pneumatic air cells, we had studied in vitro experiments.[10] On the basis of these results, clinical applications were per-

Presented at the Trilogical Society Meeting, Phoenix, AZ, April 30, 2004.

From Kyoto University, Graduate School of Medicine Kyoto, Department of Otolaryngology–Head and Neck Surgery, Syogoin, Sakyo-ku, Kyoto, Japan.

Editor's Note: This Manuscript was accepted for publication July 30, 2004.

Send Correspondence to Dr. Shin-ichi Kanemaru, Assistant Professor of Kyoto University, Graduate School of Medicine Kyoto, Department of Otolaryngology–Head and Neck Surgery, 54 Kawara-cho, Syogoin, Sakyo-ku, Kyoto, 606–8507, Japan.

DOI: 10.1097/01.mlg.0000154728.23657.3a

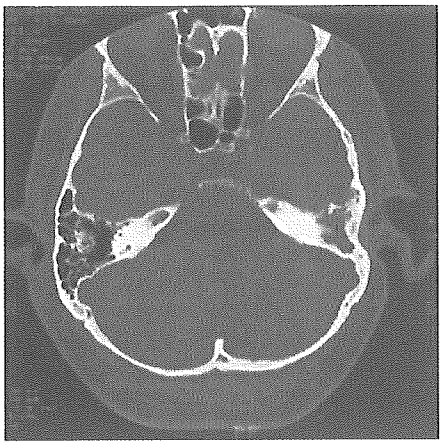

Fig. 1. Computed tomography scan image of the patient with the chronic otitis media. The development of mastoid air cells in the left side is very poor. Thick, compact bone occupies the mastoid cavity instead of mastoid air cells. This is a typical image of the cases of chronic otitis media (cholesteatoma).

formed by in situ tissue engineering. The aim of the present study was to estimate regeneration of the mastoid air cells in clinical applications.

MATERIALS AND METHODS

Artificial Pneumatic Bones

Figure 2A shows an artificial pneumatic bone made up of three-dimensional hydroxy apatite (3D-HA) with a honeycomb-like structure and a high micropore ratio of 90%. This 3D-HA is composed of calcium phosphate. Each column of this artificial pneumatic bone has a high density, as seen in a scanning electron microscopic image. Its surface is coated with collagen extracted from porcine skin with pepsin enzymatic treatment (Fig. 2B). The collagen consists of 70% to 80% of type I collagen and 20% to 30% of type III collagen. The antigenicity of these collagens is very low because of the removal of telopeptide.

Subjects

For this clinical study, 10 patients (4 males and 6 females) were randomly selected from patients with cholesteatoma, adhesive otitis media, or severe chronic otitis media. Patients ranged in age from 5 to 85 years. All but one patient, with chronic otitis media, underwent both stages of the two-stage operation. The maximum and minimum follow-up periods after the second operation were 12 and 6 months, respectively. The time interval between the first and the second stage of the operation was approximately 9 (from 8–10) months on average.

Before we started the clinical application, we got permission to use the collagen sponge as the operative material for scaffolds from the ethical committee of Kyoto University at March 2002. This collagen sponge has already been used in various operations, and the safety of it has been confirmed. The HA was the same material that had widely been used in otologic operations. The study subjects were limited to patients who fully understood the procedure and agreed to undergo this new operation by signing the informed consent paperwork.

Operative Procedures

The first-stage operation. Three patients underwent canal wall up tympanomastoidectomy. In seven patients, however, canal wall down tympanomastoidectomy with canal and attico-antrum reconstruction was performed for the purpose of complete removal of the cholesteatoma matrix. After dividing the collagen-coated 3D-HA into small pieces, it was sparsely implanted into the opened and cleaned mastoid cavity and fixed with fibrin glue (Fig. 3). During this procedure,

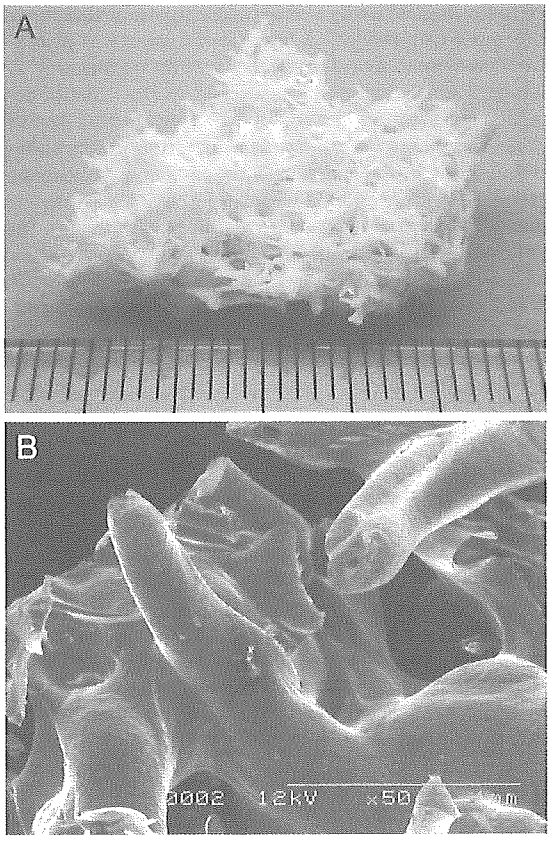

Fig. 2. (**A**) Artificial pneumatic air cells. The three-dimensional hydroxy apatite (3D-HA) is made of calcium phosphate and has a high percentage of micropores, 90%. Its surface is covered by 1% HCl atelocollagen. These materials elicit no antigenic reaction in vivo. (**B**) Scanning electron microscope image of the 3D-HA. Each column of this artificial pneumatic bone is nonporus and highly dense. Its surface is coated with collagen for easy growth of regenerative mucosa.

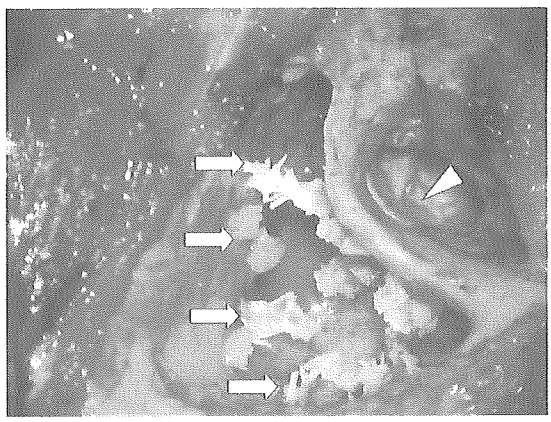

Fig. 3. Implantation of three-dimensional hydroxy apatite (3D-HA) to the newly opened mastoid cavity at the first-stage operation. External auditory canal (arrowhead). Arrows point to the opened mastoid cavity and the implanted 3D-HA.

mucosa in the mastoid cavity was treated with care so that it remained intact as much as possible.[11] A large silastic sheet was placed in the area from the tympanic cavity to the antrum for ventilation.[11] A small elastic tube, 2 mm in diameter, was inserted into the mastoid cavity for drainage and pressure regulation; this was removed after 2 or 3 weeks.

The second-stage operation. The time interval between the first and the second operation was, on average, approximately 9 months. After reopening the mastoid cavity, the presence or absence of invading soft tissue, granulation tissue, and regenerative mucosa around the implanted artificial pneumatic bones in the mastoid cavity could be assessed in this stage of the operation. When soft tissue or granulation was observed, it was removed, thereby reestablishing communication between the mastoid and tympanic cavities. In cases with partial mastoid air cell regeneration, the regions were preserved intact as much as possible (Fig. 4).

Assessment

Because there are many reports in the literature regarding the usefulness of high-resolution computed tomography (HRCT) scan images in the evaluation of the mastoid air cell system, recovery of mastoid aeration and regeneration of the pneumatic air cells of the mastoid cavity were assessed by HRCT scan images made after the first operation.[8] In the second stage of tympanoplasty, after the mastoid cavity was reopened, the surface of the 3D-HA was examined to determine whether mucosa had formed over it. In addition, a piece of implanted 3D-HA was removed as a sample specimen and investigated histologically.

RESULTS

The complete results of the 10 cases comprising this study are detailed in Table I. The table shows that in all cases, except one, soft tissue or granulation tissue had invaded into the newly opened mastoid cavity after the first-stage operation. After removal of their tissue during the second-stage operation, aeration in the mastoid cavity recovered at a high ratio. Although the regenerative ratio of mastoid air cells was only 30% (3/10) after the first operation, it increased to 60% (6/10) within 12 months after the second operation.

Pre- and Postoperative HRCT Scan Images

In all cases except one with chronic otitis media at the single-stage operation, no aeration and soft tissue density areas were observed in the mastoid and tympanic cavities in the images of preoperative HRCT scans. The development of the mastoid air cells was very poor in all cases except one.

Figures 5, 6, 7 show the HRCT scans for cases 2, 4, and 5, respectively, before and after operation with this new method. In these three cases, mastoid air cell development was very poor, aeration was absent or little, and the mastoid cavities were filled with cholesteatoma, soft tissue, or granulation tissue before surgery. However, after the first-stage operation, aeration of the mastoid cavity was recovered in all cases. Regeneration by 3D-HA of structural pneumatic air cells was especially well observed in cases 2 and 4.

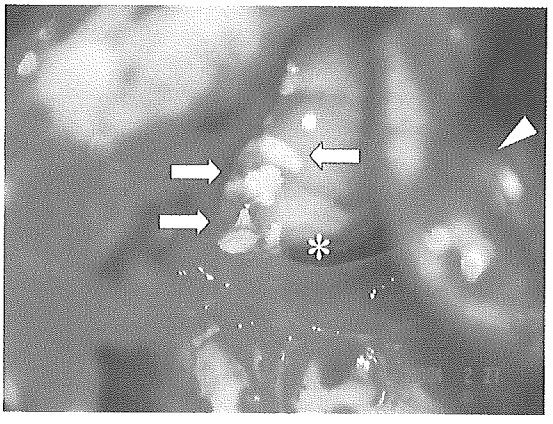

Fig. 4. Partial mastoid air cell regeneration. External auditory canal (arrowhead). Mucosa grew over the surface of the implanted three-dimensional hydroxy apatite (arrows). Antrum (asterisk).

Macroscopic Findings

Figure 8 shows the macroscopic images seen during the second-stage operation in case 2. A honeycomb-like structure and good aeration were observed in the newly formed mastoid cavity. Conversely, in case 5, a small aeration cavity was formed around the attic, but soft tissue and granulation tissue invaded the spaces of 3D-HA, and no aeration developed in the newly opened mastoid cavity. In 8 of 10 patients, soft tissue and granulation tissue invading the mastoid cavity were observed at the second operation in varying degrees. In all cases in which mastoid air cells were regenerated, mastoid cavity mucosa with blood capillaries covered the 3D-HA microscopically.

Histologic Findings

Figure 9 shows a hematoxylin-eosin stained specimen of implanted 3D-HA taken from the newly reopened mastoid cavity during the second-stage operation. Histologic regeneration of mastoid air cell mucosa with blood capillaries covering the surface of 3D-HA can be seen.

DISCUSSION

It was previously thought that the eustachian tube alone regulated ventilation and pressure in the middle ear. The function of the eustachian tube, however, is intact in some cases of cholesteatoma or adhesive otitis media. Nevertheless, even in these cases, there is a tendency toward a negative pressure balance in the middle ear after surgical intervention. It follows that there are mechanisms other than the eustachian tube involved in pressure regulation of the middle ear.

Well-developed mastoid air cells are separated by thin, bony walls and constitute many small communicating chambers. Because of this anatomic feature, the surface area is greater than that of a single cavity. These bony walls are covered with a monolayered mucosa. It is through this mucosa that mastoid air cell functions such as gas exchange, material secretion, waste excretion, and the maintenance of middle ear cavity aeration occur. Blood capillaries are abundant in the mastoid mucosa and function in gas exchange according to concentration or pressure gradients, much like the alveolar gas exchange mechanism found in the lungs.[2–7] In other words, the mastoid cavity is not only an air reservoir but also an active surface area for gas exchange.

TABLE I.
Detailed Results by Case.

Case	Age (yrs)	Sex	Diagnosis	Canal Wall Reconstruction	Soft Tissue	Aeration ($1^{st}/2^{nd}$)	Regeneration of Air Cells ($1^{st}/2^{nd}$)
1	60	F	Chole	+	+	+/+	−/−
2	73	M	Chole	+	−	+/+	+/+
3	45	F	Chole	+	+	−/+	−/+
4*	5	F	OMC	−		+	+
5	33	M	Chole	+	+	+/+	+/+
6	46	F	Chole + AOM	−	+	−/+	−/+
7	45	M	Chole	+	+	−/+	−/+
8	60	F	Chole	+	+	−/−	−/−
9	85	M	Chole	−	+	+/+	−/−
10	75	F	Chole + AOM	+	+	−/+	−/−

* Indicates the patient who was operated on only once.

Chole, OMC, AOM = indicate cholesteatoma, otitis media chronica, and adhesive otitis media, respectively; Soft tissue = indicates the presence or absence of invading soft tissue and granulation tissue in the mastoid cavity as observed at the time of the second operation; Aeration $1^{st}/2^{nd}$ = indicates a positive or negative finding for aeration in the mastoid cavity after the first/second operation on HRCT scan images; Regeneration of air cells $1^{st}/2^{nd}$ = indicates the presence or absence of regenerated mastoid air cells after the first/second operation on HRCT scan images.

Mastoidectomy is often performed in conjunction with tympanoplasty for the removal of lesions. Simple mastoid cavity plasty alone, however, is inadequate, even if the entire cavity wall is covered by mucosa, to establish or reestablish the level of transmucosal gas exchange required for ventilation and pressure regulation of the middle ear cavity. For proper pressure regulation of the middle ear, it is necessary to sufficiently expand the gas exchange surface area. Thus, tympanoplasty and mastoidectomy alone are an imperfect therapy for the treatment of intractable otitis media because they result in the absence of a mastoid air cell system, thereby precluding function. The operated ear is still left with the innate cause of the cholesteatoma or the adhesive otitis media, as well as the pathophysiologic background and therefore the tendency to develop a negative gas balance in the middle ear.[9] When traditional surgical

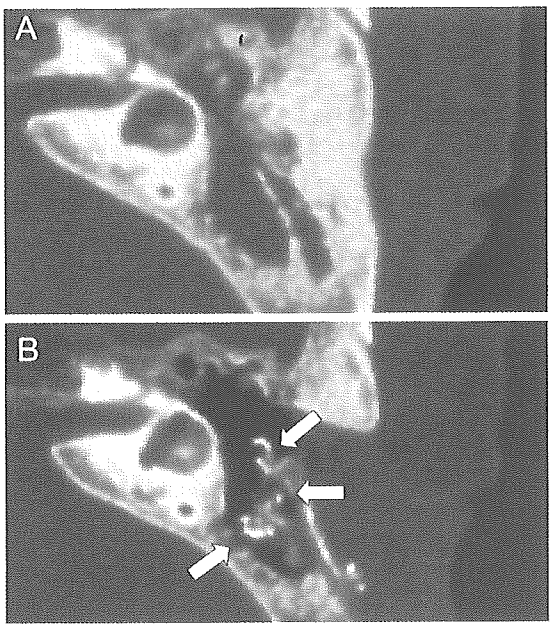

Fig. 5. Computed tomography scan images of case 2, before and after surgery. (**A**) There is no aeration in the mastoid cavity before the operation. (**B**) Six months after the second-stage operation, aeration is recovered, and the pneumatic air cells are regenerated by the three-dimensional hydroxy apatite (arrows).

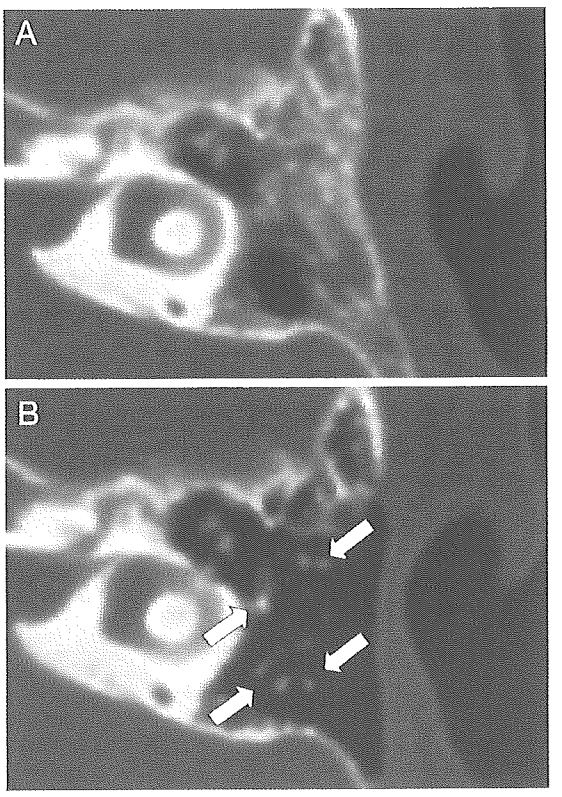

Fig. 6. Computed tomography scan images of case 4, before and after surgery. (**A**) There are few air cells and little aeration in the mastoid cavity before the operation. (**B**) Eight months after the first-stage operation, aeration is completely recovered, and the pneumatic air cells are regenerated (arrows).

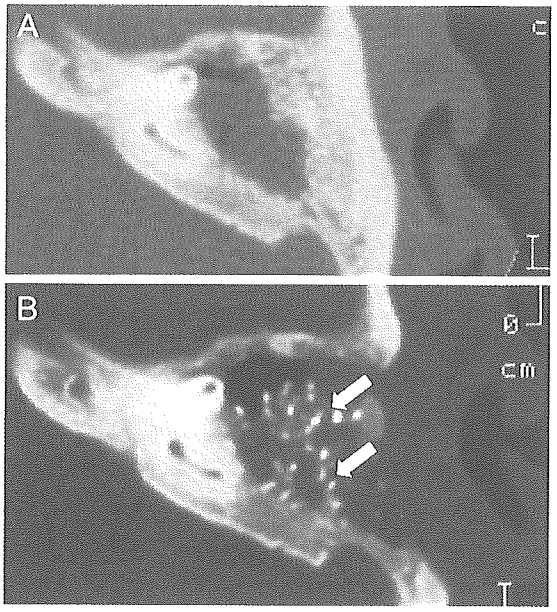

Fig. 7. Computed tomography scan images of case 5, before and after surgery. (**A**) There is no aeration in the mastoid cavity before the operation. (**B**) Eight months after the first-stage operation, aeration is partially recovered, but the pneumatic air cells are not regenerated by the three-dimensional hydroxy apatite (arrows).

techniques are performed on ears for intractable otitis media, the postoperative course is complicated by an atelectatic condition. Generation or regeneration of a functional mastoid air cell system may be required for the definitive cure of intractable otitis media.

Tissue engineering has made remarkable progress in all medical fields. According to the doctrine of tissue engineering, tissues and organs can be regenerated by manipulating three elements: cells, scaffolds, and regulation factors (Fig. 10).[12–15] The new concept of in situ tissue engineering involves local tissue regeneration achieved by the manipulation of scaffolds alone, in vivo.[16–19] Specifically, the establishment of an appropriate scaffold in vivo

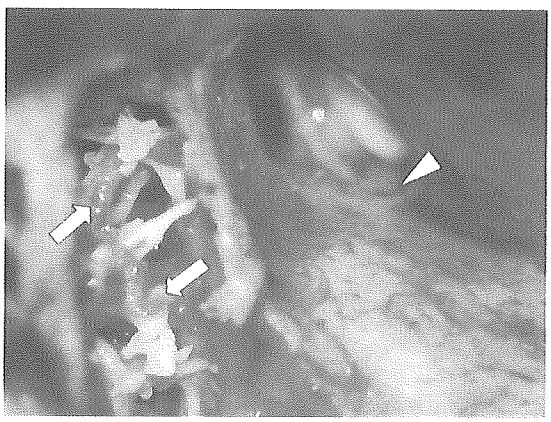

Fig. 8. A macroscopic image of the reopened mastoid cavity at the second-stage of the operation in case 2. A honeycomb-like structure and good aeration are observed in the newly formed mastoid cavity. The External auditory canal (arrowhead). Mucosa covers the implanted three-dimensional hydroxy apatite (arrows).

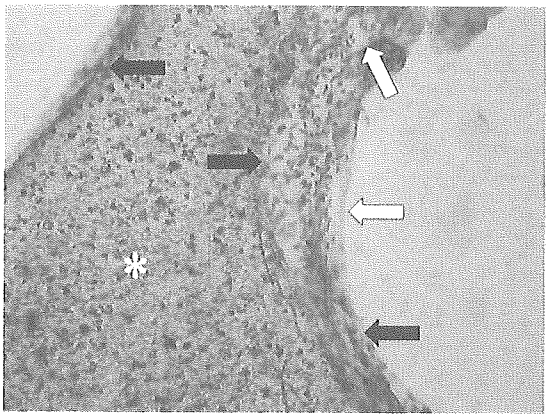

Fig. 9. Hematoxylin-eosin stained specimen of the implanted three-dimensional hydroxy apatite (3D-HA). 3D-HA (asterisk). Regenerated mucosa (black arrows). Newly organized blood capillaries (white arrows).

can induce cells and regulation factors from surrounding tissues and organs. Following this concept of in situ tissue engineering, we developed an artificial pneumatic bone to use as a scaffold for the regeneration of mastoid air cells.[10]

This artificial pneumatic bone was composed of 3D-HA and collagen. HA is a matrix widely used for the regeneration of bone in orthopedic and oral surgery.[20] We completely changed the concept of HA use from one of filling space to one of developing a functional space. Our previous in vitro study revealed that HA with a high ratio of micropore was suitable for the purpose of expanding the surface area for transmucosal gas exchange. Collagen was also found to accelerate regeneration of mucosa.[10]

This study demonstrated that mucosa can grow on the surface of implanted artificial 3D-HA in the newly opened mastoid cavity. Therefore, it is possible to generate or regenerate mastoid pneumatic air cells with viable gas exchange function by in situ tissue engineering. This tissue engineering method may be a possible treatment for intractable otitis media. Two challenges at this point are as follows:

1. Successful pneumatic air cell regeneration did not occur in all cases.

2. Does the regenerated mucosa have viable gas exchange function in practice?

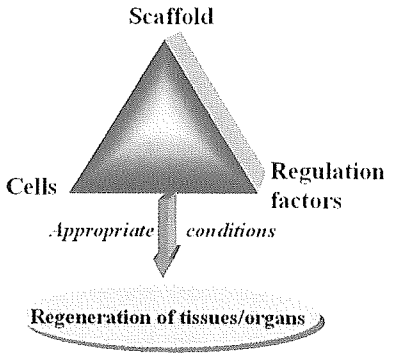

Fig. 10. Tissue engineering triad.

Problem 1

All but one case at the single-stage operation had very severe cholesteatoma or adhesive otitis media with poorly developed mastoid air cells. The patient's age seems to be one of the primary factors influencing the degree of mastoid air cell regeneration. However, no correlation was seen between the extent of disease and the degree of mastoid air cell regeneration.

The maintenance of good communication between the newly opened mastoid cavity and the tympanic cavity may well be the most important factor for the regeneration of mastoid air cells. Because the region of attic ad antrum is the only passage connecting the two cavities, and a narrow one at that, it is easily closed off by soft tissue. During the second-stage operation of this new method, it was frequently observed that this region had been closed off by the formation of a membranous barrier. The isolated mastoid cavity became filled with exudate and soft tissue with blood capillaries that invaded the spaces of the 3D-HA, thereby preventing it from serving as a honeycomb-like frame. Removing the soft tissues and reestablishing communication between the two cavities at the second-stage operation facilitated the regeneration of air cells. This was reflected in the resultant increased number of successful cases of pneumatic air cell regeneration after the second operation. Therefore, it is necessary to devise some new method for maintaining good communication between the newly opened mastoid cavity and the tympanic cavity and preventing such soft tissue invasion.

Problem 2. Recovery of mastoid cavity aeration can be assessed by HRCT images. However, it does not necessarily follow that the regenerated mucosa that grew on the surface of the 3D-HA has viable gas exchange function. We believe that the direct measurement of gas exchange function through regenerated mucosa on the surface of the 3D-HA should be performed as the next step. Further studies of this novel treatment are in order.

CONCLUSIONS

1. We used artificial pneumatic bone as a scaffold for regeneration of mastoid air cells based on the concept of in situ tissue engineering.

2. This study indicated that mucosa could grow on the surface of the implanted artificial 3D-HA within the newly opened mastoid cavity, and aeration of the cavity could be recovered in high ratio after the second operation.

3. This tissue engineering method of mastoid air cell regeneration may be a possible treatment for intractable otitis media.

Acknowledgments

The authors thank Haruo Takahashi, MD, and Seiji Hasebe, MD, for their expert advice on the conduct of this study.

BIBLIOGRAPHY

1. Sade J, Luntz M, Levy D. Middle-ear gas composition and middle-ear aeration. *Ann Otol Rhinol Laryngol* 1995;104: 369–373.
2. Ikarashi F, Nakano Y, Okura T. Pneumatization of the tympanic bulla after blockage of the ventilation route through the eustachian tube in the pig. *Ann Otol Rhinol Laryngol* 1996;105:784–790.
3. Ars B, Wuyts F, Van de Heyning P, et al. Histomorphometric study of the normal middle ear mucosa. Preliminary results supporting the gas-exchange function in the posterosuperior part of the middle ear cleft. *Acta Otolaryngol* 1997;117:704–707.
4. Takahashi H, Honjo I, Naito Y, et al. Gas exchange function though the mastoid mucosa in ears after surgery. *Laryngoscope* 1997;107:1117–1121.
5. Yamamoto Y. Gas exchange function through the middle ear mucosa in piglets: comparative study of normal and inflamed ears. *Acta Otolaryngol* 1999;119:72–77.
6. Ikarashi F, Takahashi S, Yamamoto Y. Carbon dioxide exchange via the mucosa in healthy middle ear. *Arch Otolaryngol Head Neck Surg* 1999;125:975–978.
7. Takahashi H. *The Middle Ear: The Role of Ventilation in Disease and Surgery.* Tokyo: Springer-Verlag, 2001.
8. Magrufov A, Kanemaru S, Nakamura T, et al. tissue engineering for the regeneration of the mastoid air cells: a preliminary in vitro study. *Acta Otolaryngol* 2004;124: 75–79.
9. Tanabe M, Takahashi H, Honjo I, et al. Factors affecting recovery of mastoid aeration after ear surgery. *Eur Arch Otorhinolaryngol* 1999;256:220–223.
10. Koc A, Ekinci G, Bilgili AM, et al. Evaluation of the mastoid air cell system by high resolution computed tomography: three-dimensional multiplanar volume rendering technique. *J Laryngol Otol* 2003;117:595–598.
11. Sade J. Surgical planning of the treatment of cholesteatoma and postoperative follow-up. *Ann Otol Rhinol Laryngol* 2000;109:372–376.
12. Vacanti JP. Beyond transplantation. *Arch Surg* 1988;123: 545–549.
13. Bruder SP, Fink DJ. Mesenchymal stem cells in bone development, bone repair, and skeletal regeneration therapy. *J Cell Biocem* 1994;56:283–294.
14. Vacanti CA, Upton J. Tissue-Engineered morphogenesis of cartilage and bone by means of cell transplantation using synthetic biodegradable polymer matrices. *Clin Plast Surg* 1994;21:445–462.
15. Bianco P, Robey PG. Stem cells in tissue engineering. *Nature* 2001;414:118–121.
16. Zdrahala RJ, Zdrahala IJ. In vivo tissue engineering: Part I. Concept genesis and guidelines for its realization. *J Biomater Appl* 1999;14:192–209.
17. Kropp BP, Cheng EY. Bioengineering organs using small intestinal submucosa scaffolds: in vivo tissue-engineering technology. *J Endourol* 2000;14:59–62.
18. Nakahara T, Nakamura T, Kobayashi E, et al. Novel approach to regeneration of periodontal tissues based on in situ tissue engineering: effects of controlled release of basic fibroblast growth factor from a sandwich membrane. *Tissue Eng* 2003;9:153–162.
19. Kanemaru S, Nakamura T, Omori K, et al. Recurrent laryngeal nerve regeneration by tissue engineering. *Ann Otol Rhinol Laryngol* 2003;112:492–498.
20. Mangano C, Bartolucci EG, Mazzocco C. A new porous hydroxyapatite for promotion of bone regeneration in maxillary sinus augmentation: clinical and histologic study in humans. *Int J Oral Maxillofac Implants* 2003;18:23–30.

ELSEVIER

Brain & Development 27 (2005) 233–236

BRAIN & DEVELOPMENT
Official Journal of the Japanese Society of Child Neurology

www.elsevier.com/locate/braindev

Original article

Computerized version of the Wisconsin card sorting test in children with high-functioning autistic disorder or attention-deficit/hyperactivity disorder

Emi Tsuchiya[a], Junichi Oki[b,*], Nozomi Yahara[a], Kenji Fujieda[c]

[a]*Medical Student of Asahikawa Medical College, Asahikawa, Japan*
[b]*Department of Pediatrics, Asahikawa Kosei Hospital, 1 jo 24 chome 111, Asahikawa 078-8211, Japan*
[c]*Department of Pediatrics, Asahikawa Medical College, Midorigaoka-higashi 2-1-1-1, Asahikawa 078-8510, Japan*

Received 27 January 2004; received in revised form 16 June 2004; accepted 16 June 2004

Abstract

To determine executive dysfunctions in children with autistic disorder or attention-deficit/hyperactivity disorder (ADHD), we investigated high-functioning autistic (full scale IQ score ≧70), ADHD, and control children using the computerized version of the Wisconsin Card Sorting Test. Data were obtained from 17 autistic children (16 boys and 1 girl, mean age ± SD: 12.5 ± 4.3), 22 ADHD children (20 boys and 2 girls, mean age ± SD 11.3 ± 2.6), and 25 control children (13 boys and 12 girls, mean age ± SD: 12.7 ± 3.1). Performances, indicated by mean number of categories achieved (5.4 in autistic, 6.5 in ADHD, and 8.8 in control group), total errors (38.2, 38.4, and 25.6, respectively), perseverative errors (11.4, 13.5, and 5.7), nonperseverative errors (27.1, 25.0, and 19.9), and Nelson type perseverative errors (8.9, 8.4, and 2.3), were significantly poorer in both autistic and ADHD groups than control group ($P < 0.01$). Comparing the autistic group to the ADHD group, there were no significant differences in age, gender, scores of full-scale intelligent quotient (IQ), verbal or performance IQ, number of categories achieved or errors. The ADHD group, however, showed more frequent Milner type perseverative errors than the autistic group ($P < 0.05$). The present study suggests that some kinds of executive function are more impaired in children with ADHD than in those with high-functioning autism, and that Milner type perseverative errors is useful parameter to differentiate the executive dysfunctions between autistic and ADHD children.

Keywords: Wisconsin card sorting test; High-functioning autistic disorder; Attention-deficit/hyperactivity disorder (ADHD); Executive function; Perseveration

1. Introduction

It has been proposed that some impairments of executive functions, such as those involving flexibility, set maintenance, organization, and planning, might play part in autism and attention-deficit/hyperactivity disorder (ADHD). The Wisconsin Card Sorting Test (WCST), which assesses the ability to form abstract concepts, to sustain attention, and to shift cognitive set flexibly in response to changing conceptual rules while inhibiting inappropriate responses [1–3], is one of the most commonly used tests for executive function in the school-aged population [4]. In patients with autism or ADHD, the variables reported for the standard WCST differ across studies, making comparisons between studies difficult [5].

Ozonoff et al. reported that participants with autism tended to perform better on the computerized WCST than on the standard format [2]. They suggested that the computerized version of this test would more accurately reflect executive function in autism, because it involves less social and verbal demands than the standard format. If the examiner wants to evaluate achievement under supportive conditions, to see how well the child is

* Corresponding author. Tel.: +81-166-33-7171; fax: +81-166-33-6075.
E-mail address: joki@asahikawa-kosei.jp (J. Oki).

0387-7604/$ - see front matter © 2004 Elsevier B.V. All rights reserved.
doi:10.1016/j.braindev.2004.06.008

potentially capable of performing, the computer administration format may, therefore, be preferable [6].

Although, the clinical syndrome of autism appears different from that of ADHD, children with autism may be initially diagnosed as having ADHD in clinical practice. Moreover, many children with pervasive developmental disorder not otherwise specified experience problems with attention processes, hyperactivity, acting-out behavior, and poor self-control [7]. Furthermore, in a genetic study, Smalley et al. reported that variations in a gene on 16p13 might contribute to deficits common to both ADHD and autistic disorders [8]. Clarifying the differences and similarities between autistic spectrum disorders and ADHD is of clinical significance and is also very important for clinical practice and research purposes. To investigate the possibility that executive impairment in ADHD might differ from that in autism, the present study administered the computerized version of the WCST to children with high-functioning autism, ADHD, and controls.

2. Subjects

We obtained psychiatric data from children more than 8 years of age, on the basis of the suggestion of Filley et al. that the WCST might have diagnostic utility in children as young as 8-years-old [9], although it has been recommended that caution is exercised in children under 10 [10]. The Wechsler Intelligence Scale for Children-Revised (WISC-R; 1974) or WISC-Third Edition (WISC-III; 1991) were used to measure general intellectual ability. We obtained informed consent for all participants before their enrollment in the protocol.

2.1. High-functioning autistic group

Seventeen children (16 boys and 1 girl) with high-functioning autism were recruited for participation through the Department of Pediatrics, Asahikawa Medical College and the Asahikawa Kosei Hospital. Diagnosis was verified using DSM-IV (American Psychiatric Association, 1994) criteria. Average age of subjects was 12.5±4.3 (mean± SD). Wechsler's intelligence test showed mean scores and standard deviation as follows: full-scale intelligence quotient (FSIQ), 92.3±12.5; verbal IQ (VIQ), 90.8± 17.8; performance IQ (PIQ), 96.7±12.1.

2.2. ADHD group

Twenty-two children (20 boys and 2 girls) with ADHD were recruited for participation through the above departments. Diagnosis was verified using DSM-IV. All, but one subject was classified as having attention-deficit/hyperactivity disorder, combined type. Average age of subjects was 11.3±2.6 and mean IQ scores were as follows: FSIQ, 98.3±15.1; VIQ, 97.8±16.7; PIQ, 96.9±16.6. No statistically significant differences of FSIQ, VIQ, PIQ, race, socioeconomic status, or gender were found between the high-functioning autistic group and ADHD group.

2.3. Control group

Twenty-five children (13 boys and 12 girls) were recruited for control. Average age of controls, who were also screened for medication use and history of psychiatric illness, was 12.7±3.1 (SD). They have attended school without any problems concerned with relationship to schoolmates or academic works. In control group, there were no significant sex differences in WCST and IQs. No statistical differences were observed between autistic, ADHD and control groups with respect to age.

3. Methods

Each participant was administered a computerized version (version 1.00 for Windows 95) of the WCST. The WCST consists of four stimulus cards that vary along three dimensions (color, shape, and number). Participants are given 128 cards that vary along the same dimensions and are asked to match the cards in the deck with one of the fourth stimulus cards. The computer screen displays '○' for correct placement of a card and '×' for incorrect placement, but does not reveal the sorting strategy, which must be inferred from the feedback provided. Once 10 consecutive cards are categorized correctly, the sorting principle changes without warning or comments from the examiner and all sorts made according to the previous strategy then receive negative feedback. This procedure continues until all 128 cards are placed. In addition to yielding total error scores, this technique yields separate measurements for perseverative and nonperseverative errors and for the number of sorting categories achieved. Milner type perseverative errors were defined as those that were correct on the immediately preceding stage of the test; all other perseverative errors were defined as Nelson type [11–13].

As ages, number of categories achieved, and errors were equally distributed using an F-test, we used a t-test for comparison of each pair of groups (autistic versus control, ADHD versus control, autistic versus ADHD). Results were considered statistically significant if the P value was less than 0.05.

4. Results

Results of the computerized version of the WCST are shown in Table 1.

Table 1
Group mean performance and errors on the computerized WCST (mean±SD)

Source	Autistic group (n=17)	ADHD group (n=22)	Control group (n=25)
Categories achieved	5.4±2.6**	6.5±1.9**	8.8±1.5
Total errors	38.2±16.6**	38.4±13.5**	25.6±6.0
Perseverative errors	11.1±7.4**	13.5±8.3**	5.7±3.6
Milner type	2.2±2.0	5.1±4.7*[a]	3.4±2.8
Nelson type	8.9±7.8**	8.4±7.8**	2.3±3.0
Non-perseverative error	27.1±12.3**	25.0±6.6**	19.9±4.0

*$P<0.05$, **$P<0.01$ when compared to the control group.
[a] $P<0.05$ when compared to the autistic group.

4.1. Autistic group versus control

In comparisons between the high-functioning autistic group and the control group, there were significant differences in the following: number of categories achieved, $t(40)=-4.52$, $P<0.01$; total errors, $t(40)=3.41$, $P<0.01$; perseverative errors, $t(40)=3.07$, $P<0.01$; Nelson type perseverative errors, $t(40)=3.77$, $P<0.01$; and nonperseverative errors, $t(40)=2.66$, $P<0.01$. The autistic group performed less well than the control group. In contrast, there was no significant difference between two groups regarding the number of Milner type perseverative errors.

4.2. ADHD versus control

When these two groups were compared, significant differences in the following parameters were also observed: number of categories achieved, $t(45)=-4.51$, $P<0.01$, total errors, $t(45)=4.21$, $P<0.01$; perseverative errors, $t(45)=4.15$; Nelson type errors, $t(45)=3.55$, $P<0.01$; and nonperseverative errors, $t(45)=3.17$, $P<0.01$. The ADHD group performed less well than the control group. In contrast, there was no significant difference in the number of Milner type perseverative errors.

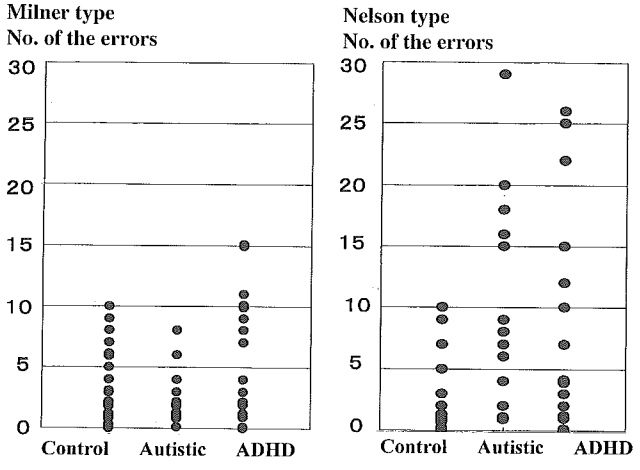

Fig. 1. Distributions of the preservative errors of Milner and Nelson type among control, autistic, and ADHD groups.

4.3. Autistic versus ADHD group

Although there were no significant differences in age, gender, scores of FSIQ, VIQ or PIQ, number of categories achieved or errors, the ADHD group showed more frequent perseverative errors of Milner type than the autistic group [$t(37)=2.31$, $P<0.05$] (Fig. 1). There was a trend towards larger Milner type perseverative errors in ADHD group compared with control and autistic groups.

5. Discussion

As executive dysfunction has been reported in the developmental, psychiatric and neurological disorders, it has been proposed that autistic subjects suffer from primarily deficiencies in flexibility and planning, and that ADHD subjects have difficulties of sustaining attention and inhibiting behavior [2,14,15]. The WCST, one of the tests reflecting executive function, is thought to measure set maintenance skills, the ability to flexibly modify incorrect strategies, and to inhibit incorrect responses. The test provides several dependent variables. The number of categories achieved and errors made are calculated as measures of conceptual problem solving that highlight the subject's understanding of the nature of the categorization task. The number of perseverative errors is thought to be the best predictor of prefrontal dysfunction [4,11]. Pennington and Ozonoff [15] reviewed research on executive functions and described the WCST as being more consistently and severely impaired in high-functioning autism than in ADHD. In contrast, Minshew et al. [16] and Liss et al. [17] reported no significant differences in terms of perseverative errors on the WCST between high-functioning autistic subjects and controls after the variance due to verbal IQ was accounted for.

In order to eliminate the influence of verbal cognitive function, we used the computerized version of the WCST in the present study. This study revealed that both autistic and ADHD subjects showed greater impairments in categories achieved and perseverative, nonperseverative errors than controls. These results were consistent with those of Seidman et al. [18]. As Milner type perseverative errors reflect dysfunction in shifting cognitive set flexibly in response to changing conceptual rules, we had speculated that children with autism would show more Milner type perseverative errors than those with ADHD. However, children with ADHD made a greater number of Milner type perseverative errors than those with autism in the present study, despite no statistical significant difference in age, gender, race, FSIQ, VIQ, or PIQ. Dawson et al. found that the severity of autistic symptoms was strongly and consistently correlated with performance in the medial

temporal lobe task, but not the dorsolateral prefrontal task [19]. Moreover, adult patients with early frontal lesions came to psychiatric attention, but did not appear to demonstrate autistic symptoms [20]. We, therefore, speculated that ADHD children would show more deficient in flexibility than high-functioning autistic children, although the present study indicated that both groups showed some degree of executive dysfunction.

6. Conclusion

The computerized version of the WCST revealed similar degree of executive dysfunction in both children with autism and ADHD compared with control subjects. However, ADHD subjects showed more Milner type perseverative errors. These results suggest that children with ADHD show more deficient in flexibility than high-functioning autistic children. The authors, therefore, recommend that perseverative errors on the WCST should be categorized as Milner or Nelson type in order to discriminate the executive dysfunctions between autism and ADHD.

References

[1] McBurnett K, Harris SM, Swanson JM, Pfiffner LJ, Tamm L, Freeland D. Neuropsychological and psychophysiological differentiation of inattention/overactivity and aggression/defiance symptom groups. J Clin Child Psychol 1993;22:165–71.
[2] Ozonoff S. Reliability and validity of the Wisconsin Card Sorting Test in studies of autism. Neuropsychology 1995;9:491–500.
[3] Schmitz M, Cadore L, Paczko M, Kipper L, Chaves M, Rohde LA, et al. Neuropsychological performance in DSM-IV ADHD subtypes: an exploratory study with untreated adolescents. Can J Psychiatry 2002;47:863–9.
[4] Ozonoff S, Pennington BF, Rogers SJ. Executive function deficits in high-functioning autistic individuals: relationship to theory of mind. J Child Psychol Psychiatry 1991;32:1081–105.
[5] Sergeant JA, Geurts H, Oosterlaan J. How specific is a deficit of executive functioning for attention-deficit/hyperactivity disorder? Behav Brain Res 2002;130:3–28.
[6] Goodlin-Jones BL, Solomon M. Contributions of psychology. In: Ozonoff S, Rogers SJ, Hendren RL, editors. Autism spectrum disorders. Washington, DC, London: American Psychiatric Publishing, Inc.; 2003. p. 55–85.
[7] Luteijn EF, Serra M, Jackson S, Steenhuis MP, Althaus M, Volkmar F, et al. How unspecified are disorders of children with a pervasive developmental disorder not otherwise specified? Eur Child Adolesc Psychiatry 2000;9:168–79.
[8] Smalley SL, Kustanovich V, Minassian SL, Stone JL, Ogdie MN, McGough JJ, et al. Genetic linkage of attention-deficit/hyperactivity disorder on chromosome 16p13, in a region implicated in autism. Am J Hum Genet 2002;71:959–63.
[9] Filley CM, Young DA, Reardon MS, Wilkening GN. Frontal lobe lesions and executive dysfunction in children. Neuropsychiatry Neuropsychol Behav Neurol 1999;12:156–60.
[10] Chelune GJ, Baer RA. Developmental norms for the Wisconsin Card Sorting Test. J Clin Exp Neuropsychol 1986;8:219–28.
[11] Milner B. Effects of different brain lesions on card sorting. Arch Neurol 1963;9:100–10.
[12] Nelson HE. A modified card sorting test sensitive to frontal lobe defects. Cortex 1976;12:313–24.
[13] Kashima H, Kato M. Tests for frontal function-pattern of frontal dysfunction and its assessment (in Japanese). Shinkei Kenkyu no Shinpo (Tokyo) 1993;37:93–110.
[14] Ozonoff S, Jensen J. Brief report: specific executive function profiles in three neurodevelopmental disorders. J Autism Dev Disord 1999;29:171–7.
[15] Pennington BF, Ozonoff S. Executive functions and developmental psychopathology. J Child Psychol Psychiatry 1996;37:51–87.
[16] Minshew NJ, Goldstein G, Muenz LR, Payton JB. Neuropsychological functioning in nonmentally retarded autistic individuals. J Clin Exp Neuropsychol 1992;14:749–61.
[17] Liss M, Fein D, Allen D, Dunn M, Feinstein C, Morris R, et al. Executive functioning in high-functioning children with autism. J Child Psychol Psychiatry 2001;42:261–70.
[18] Seidman LJ, Biederman J, Faraone SV, Weber W, Ouellette C. Toward defining a neuropsychology of attention deficit-hyperactivity disorder: performance of children and adolescents from a large clinically referred sample. J Consult Clin Psychol 1997;65:150–60.
[19] Dawson G, Meltzoff AN, Osterling J, Rinaldi J. Neuropsychological correlates of early symptoms of autism. Child Dev 1998;69:1276–85.
[20] Price BH, Daffner KR, Stowe RM, Mesulam MM. The compartmental learning disabilities of early frontal lobe damage. Brain 1990;113:1383–93.

Available online at www.sciencedirect.com

SCIENCE DIRECT®

Virology 338 (2005) 173 – 181

VIROLOGY

www.elsevier.com/locate/yviro

Induction of suppressor of cytokine signaling-3 by herpes simplex virus type 1 confers efficient viral replication

Shin-ichi Yokota[a], Noriko Yokosawa[a], Tamaki Okabayashi[a], Tatsuo Suzutani[b], Nobuhiro Fujii[a,*]

[a]*Department of Microbiology, Sapporo Medical University School of Medicine, South-1, West-17, Chuo-ku, Sapporo, 060-8556 Hokkaido, Japan*
[b]*Department of Microbiology, Fukushima Medical University School of Medicine, Fukushima 960-1295, Japan*

Received 25 March 2005; returned to author for revision 21 April 2005; accepted 23 April 2005
Available online 6 June 2005

Abstract

We showed previously that infection of herpes simplex virus type 1 (HSV-1) rapidly induced the suppressor of cytokine signaling-3 (SOCS3), a host negative regulator of the JAK/STAT pathway, in the amnion cell line FL. Thus, HSV-1 suppresses the interferon (IFN) signaling pathway at the step of IFN-induced phosphorylation of janus kinases during an early infection stage. In the present study, we examined SOCS3 induction by HSV-1 infection in several types of human cell lines. FL cells and the T-cell line CCRF-CEM strongly induced SOCS3 during HSV-1 infection. The virus rapidly propagated in both cell lines and produced a lytic infection. On the other hand, the monocytic cell lines U937 and THP-1, and the B-cell line AKATA showed neither SOCS3 induction nor suppression of IFN-induced STAT1 phosphorylation during HSV-1 infection. These cell lines resulted in a persistent or prolonged infection, which continuously produced a low titer of infectious virus. The induction of SOCS3 by HSV-1 should occur via STAT3 activation immediately after HSV-1 infection. SOCS3 induction was inhibited by the addition of a Jak3 inhibitor WHI-P131. Treatment with WHI-P131 or transfection of antisense oligonucleotides specific for SOCS3 dramatically suppressed replication of HSV-1 in FL cells. The suppression of viral replication by WHI-P131 was released in the presence of neutralizing anti-IFN-α and anti-IFN-β antibodies. In conclusion, suppression of IFN signaling by HSV-1-induced SOCS3 is required for efficient replication and lytic infection of HSV-1. The SOCS3 induction varied among cell lines, indicating that it is an important factor determining the cell type specificity of efficient HSV-1 replication.

Keywords: Herpes simplex virus type 1; Interferon; SOCS3; Viral replication; Cell signal transduction; Protein kinase inhibitor; Jak3 inhibitor; STAT3

Introduction

Cells have various defense mechanisms that protect them from viral infection. Interferon (IFN) is induced by viral infection and plays an important role in defending the host cell from viral attack. When IFN binds to specific cell surface receptors on the host cells, it promotes the antiviral state through induction or activation of the 2′,5′-oligoadenylate synthetase (2-5AS)/RNase L system, the double-stranded RNA-activated protein kinase (PKR), and the MxA protein (Fujii, 1994; Samuel, 2001; Sen and Ransohoff, 1993). Signal transduction by IFN is mediated through the JAK/STAT pathway which consists of janus kinases (JAK), protein tyrosine kinases that interact with the intracellular domains of various receptors, and the STAT family proteins, transcription factors that are activated through phosphorylation by JAK. The JAK/STAT pathway also transduces various cytokine signals. There are four JAK proteins (Jak1, Jak2, Jak3, and Tyk2) and seven STAT proteins (STAT1 to 4, STAT5a, STAT5b, and STAT6) (Aaronson and Horvath, 2002; Darnell et al., 1994; Leonard and O'Shea, 1998; O'Shea et al., 2002). Each cytokine employs a particular combination of the JAK and STAT proteins, which in turn determines the specificity of the cytokine responses. For instance, Jak1 and Tyk2 are associated with the IFN-α/β receptor complex. These JAK proteins are activated by phosphorylation after IFN-α/β binds to its receptor, and they phosphorylate STAT1 and STAT2. Phosphorylated STAT1 and phosphorylated STAT2 can bind to IRF-9/p48/ISGF3γ,

* Corresponding author. Fax: +81 11 612 5861.
E-mail address: fujii@sapmed.ac.jp (N. Fujii).

0042-6822/$ - see front matter © 2005 Elsevier Inc. All rights reserved.
doi:10.1016/j.virol.2005.04.028

to form the transcription factor ISGF3, which then translocates into the nucleus and binds to IFN-stimulated response elements in the promoters of IFN-inducible genes (Darnell et al., 1994; Goodbourn et al., 2000; Samuel, 2001).

According to recent reports, herpes simplex virus type 1 (HSV-1) suppresses the IFN signaling pathway at multiple sites in order to evade host defense mechanisms. We reported that IFN-induced JAK phosphorylation was inhibited in FL cells during the early infection stages of HSV-1 (Yokota et al., 2001) and suppressor of cytokine signaling-3 (SOCS3), which is a host negative regulator of the JAK/STAT pathway, was rapidly induced under these conditions (Yokota et al., 2004b). The UL41 gene product (virion host shutoff protein) contributes to IFN resistance (Suzutani et al., 2000). Chee and Roizman (2004) reported that HSV-1-blocked-IFN signaling in part by reduced levels of Jak1 and STAT2 proteins through the action of the UL41 gene product. In addition, HSV-1 suppresses IFN production. Melroe et al. (2004) reported that HSV-1 inhibited the production of IFN-β, which is partly mediated by degradation of IFN regulatory factor 3 (IRF-3). The immediate early protein ICP0 contributes to this. Lin et al. (2004) reported that ICP0 inhibited IRF-3- and IRF-7-mediated gene activation, including IFN-β production, without degradation of proteins, such as IRF-3, CBP, and TBK-1. They also showed that hyperphosphorylation of IRF-3 did not occur during HSV-1 infection. In contrast, our previous report showed that phosphorylation of IRF-3 and induction of IFN-β mRNA occurred during HSV-1 infection (Yokota et al., 2004b). Mogensen et al. (2004) reported that production of proinflammatory cytokines, including IFN-α/β, was suppressed by HSV-1, and the suppression was caused by participation of the immediate early gene products, ICP4 and ICP27. Suppression of IFN-induced effectors by HSV-1 has been also reported. Phosphorylated eIF-2α, which shuts off protein synthesis, is dephosphorylated by cooperation of viral $\gamma_1$34.5 protein and host protein phosphatase 1α (He et al., 1997). So, the IFN-induced protein synthesis shutoff is released by HSV-1. In addition to $\gamma_1$34.5, the late gene Us11 also contributes to IFN resistance (Mulvey et al., 2004). Promyelocytic leukemia protein (PML), which forms nuclear body ND10 and contributes to anti-viral activity, is degraded by viral ICP0 (Chee et al., 2003; Everett et al., 1998).

Previously, we showed that SOCS3 was rapidly induced in FL cells by HSV-1 infection (Yokota et al., 2004b). The induced SOCS3 protein reaches maximal levels around 1 to 2 h post-infection and inhibits IFN-induced phosphorylation of JAK. We consider this event to be crucial in HSV-1 inhibition of IFN system because it occurs most rapidly after infection as compared to the strategies described above which should take at least several hours to occur. The SOCS family proteins are STAT-induced STAT inhibitors that provide negative feedback regulation of the JAK/STAT pathway. These proteins commonly share an N-terminal region of variable length, a central src homology 2 (SH2) domain, and a C-terminal SOCS box. SOCS proteins are generally expressed at low levels in cells and their gene transcription is induced by various cytokines that activate the JAK/STAT pathway (Alexander, 2002; Cooney, 2002; Krebs and Hilton, 2001; Yasukawa et al., 2000). To date, eight SOCS family proteins (SOCS1 to 7 and CIS) have been identified. Of these, SOCS1 and SOCS3 are reported to inhibit signal transduction by IFN (Bode et al., 2003; He et al., 2003; Sen and Ransohoff, 1993; Song et al., 1998; Yokota et al., 2004b). SOCS3 has been reported to inhibit various cytokines including IFNs, such as interleukin-1 (IL-1), IL-2, IL-3, IL-4, IL-6, growth hormone, prolactin, insulin, oncostatin M, leptin, erythropoietin, and ciliary neurotropic factor (Alexander, 2002; Cooney, 2002; Krebs and Hilton, 2001; Yasukawa et al., 2000). SOCS3 associates with cytokine receptors and inhibits activation, namely phosphorylation, of JAKs (Nicholson et al., 2000; Schmitz et al., 2000). SOCS1 directly interacts with JAK and inhibits their enzymatic activity (Yasukawa et al., 1999).

Our previous paper described induction of SOCS3 in FL cells (Yokota et al., 2004b). Currently, it is unclear whether the induction of SOCS3 by HSV-1 is general phenomenon in other cell types or not. In the present study, we examined SOCS3 induction in various cell lines and found that the inducibility of SOCS3 was correlated with rapid viral replication in the early stages of infection.

Results

Inducibility of SOCS-3 by HSV-1 varies among cell lines and correlates with viral replication

Previously, we described SOCS3 induction during HSV-1 infection in FL cells (Yokota et al., 2004b). In the present study, we examined the mRNA expression of JAK/STAT negative regulators in various types of cell lines, in the presence or absence of HSV-1 infection (Fig. 1A). FL and CCRF-CEM showed a dramatic increase in SOCS3 mRNA following virus infection (9.27-fold and 15.30-fold, respectively). TALL-1 showed a weak increase (4.70-fold) upon infection. U937, THP-1, and AKATA did not show any SOCS3 induction. Protein expression levels of SOCS3 were consistent with the results of semi-quantitative reverse transcription-polymerase chain reaction (RT-PCR) (Fig. 1B). Induction of SOCS3 protein was also observed in FL cells (4.46-fold compared to untreated control) and CCRF-CEM cells (5.33-fold). TALL-1 showed very weak increase (1.65-fold). However, the other cell lines express SOCS3 protein, under normal culture condition, they did not show significant changes in SOCS3 protein levels. The basal expression levels SOCS3 were 1.19 (TALL-1), 0.79 (CCRF-CEM), 1.10 (AKATA), 1.05 (THP-1), and 1.47 (U937), relative to level in FL cells, which was set as 1.00. The quantitative values were mean values deduced from three time experiments. CIS mRNA was downregulated in TALL-1 and CCRF-CEM and upregulated in THP-1 cells by HSV-1 infection. SOCS1 mRNA was observed in AKATA and U937 cells, and their expression levels did not change by

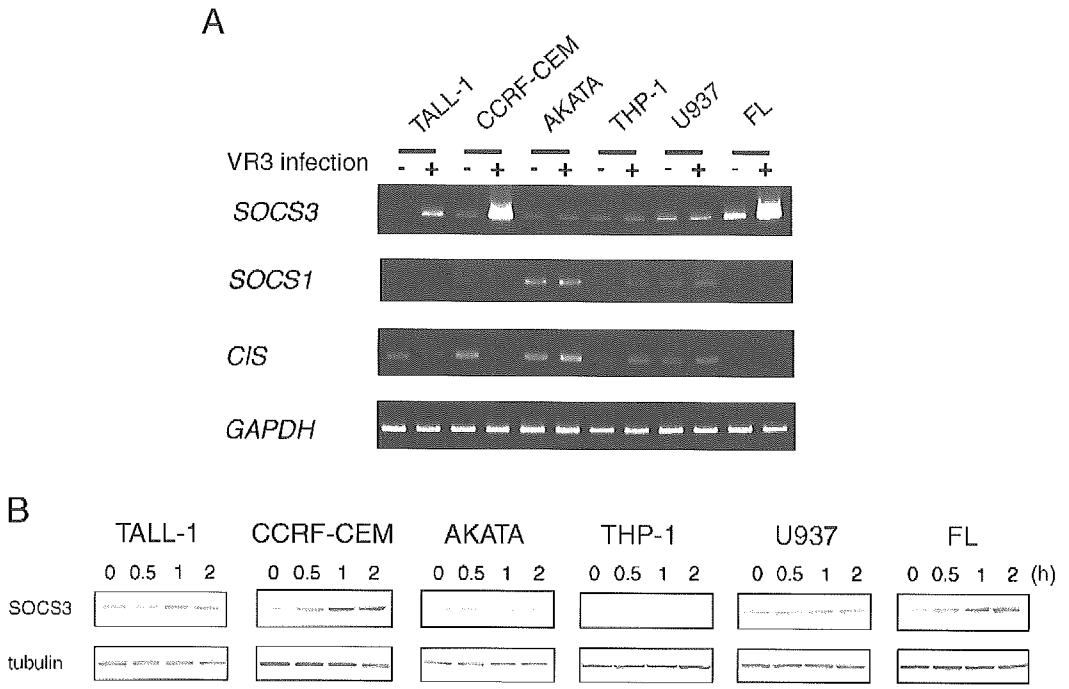

Fig. 1. Effect of HSV-1 infection on expression of SOCS family genes in various cell lines. (A) mRNA levels determined by RT-PCR. TALL-1, CCRF-CEM, AKATA, THP-1, U937, and FL cells were infected with HSV-1 strain VR3 at an MOI of 5. After 1 h of infection, cells were harvested. Total cellular RNA was extracted and assessed by semi-quantitative RT-PCR using specific primer sets for detecting SOCS3, SOCS1, and CIS. GAPDH was carried out as a control. The PCR products were analyzed by 2%(w/v) agarose electrophoresis. (B) Protein levels determined by Western blotting. Infected cells were harvested at various times after infection as indicated for each lane. Cell lysates were assessed by Western blotting with an anti-SOCS3 antibody. β-tubulin was examined as a control. Fifty micrograms and 5 μg proteins were applied to SDS-PAGE for analysis of SOCS3 and β-tubulin, respectively.

HSV-1 infection. SOCS1 expression was slightly upregulated by HSV-1 infection in THP-1 cells. Neither SOCS1 nor CIS mRNA was detected in FL cells. Viral infection of cells was determined by immunofluorescence microscopy. All cells so far observed were positive for anti-HSV-1 antibody (Fig. 2). Consistent with the induction of SOCS3, IFN-α-induced STAT1 phosphorylation was almost completely inhibited in FL and CCRF-CEM cells by HSV-1 infection (Fig. 3). The phosphorylation was partially inhibited in TALL-1 cells and the inhibition was not observed in U937, THP-1, and AKATA cells by HSV-1 infection (Fig. 3). In FL and CCRF-CEM cells, HSV-1 efficiently replicated (virus reached more than 10^7 pfu/ml in culture medium during a few days of infection) and then produced a lytic infection (Table 1). Cytopathic effects were not observed in TALL-1. Only weak cytopathic effects were observed in U937, THP-1, and AKATA. The latter four cell lines produced low titers (about 10^4 to 10^5 pfu/ml) of infectious virus in the culture medium, even though HSV-1 had infected all cells in the culture as observed by immunofluorescence microscopy (Fig. 2). TALL-1, U937, and THP-1 infected with HSV-1 were able to be maintained by repetitive subculture, however, infected AKATA cells died approximately 10 days after infection without high titer virus production. These results suggest that HSV-1 rapidly replicated and caused lytic infections in cells which strongly induce SOCS3. In contrast, HSV-1 did not replicate efficiently and produced a prolonged or persistent infection with low titer virus production in cells which showed weak or little induction of SOCS3.

Suppression of SOCS3 expression by an antisense oligonucleotide results in suppressed virus replication

To examine the contribution of SOCS3 to HSV-1 replication, we used an antisense oligonucleotide specific for SOCS3. After transfection of SOCS3 antisense oligonucleotide or its negative control oligonucleotide, cells were challenged with the virus at an MOI of 1. The virus titers after 24 h of infection were determined by the plaque-forming assay. At high concentrations (500 nM) of oligonucleotide, basal and HSV-1-induced levels of SOCS3 mRNA expression were efficiently suppressed (Fig. 4A). Under these conditions, viral replication was dramatically suppressed (about 10^3 pfu/ml reduction) (Fig. 4B). Control oligonucleotides did not have such effect. Similar results were observed for another high responder cell, CCRF-CEM. However, CCRF-CEM showed relatively weak suppression of SOCS3 expression and viral replication (about 10^2 pfu/ml reduction) by transfection of antisense oligonucleotides compared to FL cells (data not shown). This should be due to less transfection efficacy in CCRF-CEM cells, which were suspension cells, than in FL cells, which were adherent cells. On the other hand, we observed that virus replication in U937 and THP-1, which did not show SOCS3 induction by HSV-1 infection, did not interfere by the transfection of

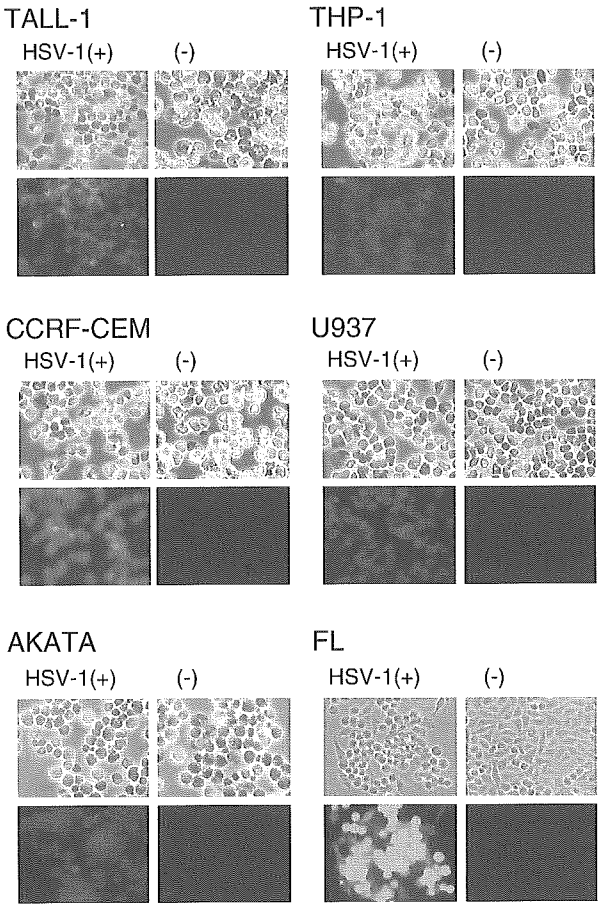

Fig. 2. Immunofluorescence microscopic analysis of the presence of virus in cells infected with HSV-1. TALL-1, CCRF-CEM, AKATA, THP-1, U937, and FL cells were infected with HSV-1 VR3 at an MOI of 5. After 24 h of infection, cells were fixed with methanol and stained with fluorescence-labeled anti HSV-1 antibody. HSV-1 (+): HSV-1 infected cells; (−): uninfected control cells; upper panels: phase contrast; lower panels: fluorescence.

SOCS3 antisense oligonucleotides (data not shown). These results indicate that induction of SOCS3 by HSV-1 infection contributed to the efficiency of viral replication.

Inhibition of Jak3 activation results in suppression of viral replication

Expression of human SOCS3 is controlled by the transcription factor, STAT3, as well as murine one (He et al., 2003) . We observed that STAT3 was rapidly phosphorylated after HSV-1 infection in FL cells and CCRF-CEM cells (Fig. 5). In contrast, THP-1 cells did not show induction of SOCS (Fig. 1) and phosphorylation of STAT3 (Fig. 5) by HSV-1 infection. STAT3 is phosphorylated by Jak3 and Jak3 is independent to IFN signaling, so we used an inhibitor of Jak3 (WHI-P131) in order to suppress SOCS3 expression. We confirmed that WHI-P131 did not influence on IFN-α-induced phosphorylation of Jak1 and Tyk2, and IFN-γ-induced phosphorylation of Jak1 and Jak2 (data not shown). FL cells were pretreated with WHI-P131 for 30 min, and then virus challenged. WHI-P131 at a concentration of 50 μg/ml required for almost complete suppression of basal and HSV-1-induced SOCS3 mRNA levels, as detected by semi-quantitative RT-PCR (Fig. 6A) and Western blotting (Fig. 6B). In the absence of WHI-P131, HSV-1 infection blocked IFN-α-induced Jak1 phosphorylation. In the presence of WHI-P131, HSV-1 was no longer able to suppress IFN-induced Jak1 phosphorylation, although basal protein levels of Jak1 were significantly decreased by WHI-P131 (Fig. 6C). Viral replication was dramatically suppressed in the presence of WHI-P131 (Fig. 6D). The suppression by WHI-P131 was more clearly observed in HSV-1 infection at an MOI of 1 than at an MOI of 5. The negative control compound, WHI-P258, did not show any effect on virus titer compared to controls.

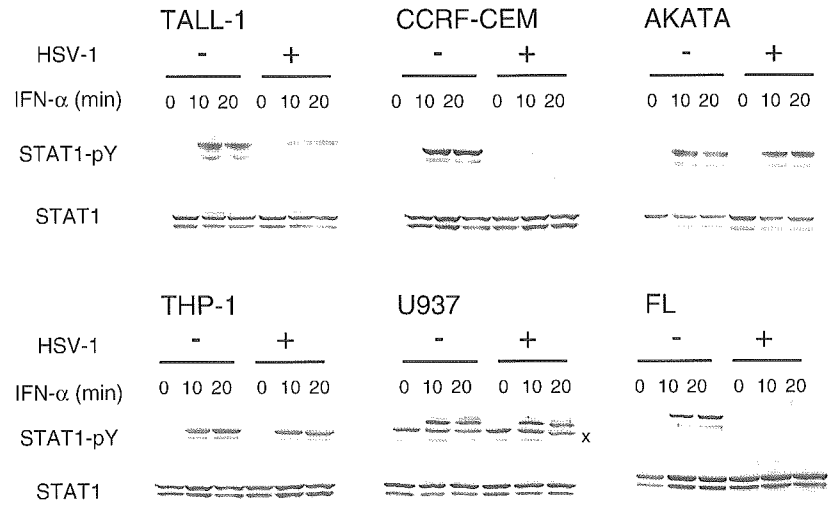

Fig. 3. Effect of HSV-1 infection on IFN-α-induced STAT1 phosphorylation. TALL-1, CCRF-CEM, AKATA, THP-1, U937, and FL cells were infected with HSV-1 strain VR3 at an MOI of 5. After 2 h of infection, cells were treated with 1000 IU/ml IFN-α for 10 or 20 min. Cells were lysed and assessed by Western blotting using anti-Tyr-phosphorylated STAT1 (STAT1-pY) and anti-STAT1 antibodies. x in the U937 panel indicates non-specific bands.